Optics Communications 335 (2015) 73–77

Contents lists available at ScienceDirect

Optics Communications

journal homepage: www.elsevier.com/locate/optcom

Label-free optical sensor by designing a high-Q photonic crystal ring–slot structure

Lijun Huang [a,b], Huiping Tian [a,*], Jian Zhou [a], Qi Liu [a], Pan Zhang [a], Yuefeng Ji [a]

[a] State Key Laboratory of Information Photonics and Optical Communications, School of Information and Communication Engineering, Beijing University of Posts and Telecommunications, Beijing 100876, China
[b] Department of Physics and Information Engineering, Huaihua University, Huaihua, Hunan 418008, China

ARTICLE INFO

Article history:
Received 24 June 2014
Received in revised form
20 August 2014
Accepted 5 September 2014
Available online 18 September 2014

Keywords:
Optical sensing and sensors
Ring–slot structure
Coupled resonators
Resonators
Photonic crystals

ABSTRACT

We propose a label-free refractive index (RI) sensor based on a high-*Q* photonic crystal (PhC) ring–slot resonator. The proposed device consists of a ring–slot cavity, in which light is coupled input and output by using a PhC line defect waveguide (W_1). By using two dimensional finite-difference time-domain (2D –FDTD) simulation, we show that a *Q*-factor as high as 10^7 is achieved when the width (w) of ring–slot equals to $0.20a$ and the radius of center air hole inner ring–slot equals to $0.34a$. Even though the refractive index (RI) equals to 1.330 (water surroundings) at telecom wavelength range, *Q* of $\sim$11477.3 can also be achieved when the width of ring–slot equals to $0.28a$. The RI sensitivity (S) equals to 160 nm/RIU (refractive index unit) and the detect limit (DL) of 8.75×10^{-5} RIU is obtained. These suggest that the design is a promising candidate for label-free biosensing in medical diagnosis, life science and environmental monitoring.

1. Introduction

High quality factor (*Q*-factor) micro-cavities [1–3], due to the narrow resonance line width and long photon storage time, are prominent candidates for sensors with enhanced detection sensitivity [4–10] and accurate detection limitation [10]. Several micro-cavities such as micro-ring cavities [4,11–20], micro-toroids [21], fiber bragg grating/Fabry–Perot (FBG/FP) cavity [22], photonic crystals [5,6,9,23–39] had been extensively studied in the past few decades. A high *Q* micro-ring cavity is recent demanded for a number of applications [10], such as label-free RI sensor, because high *Q* of the resonator can decrease the impact of noise on the detection of the resonance wavelength. Vos et al. [14] proposed a label-free biosensor based on micro-ring cavities in Silicon-on-Insulator (SOI), and they used the avidin/biotin high affinity couple to demonstrate good repeatability and detection of protein concentrations down to 10 ng/ml, and this sensor has a *Q* factor of 20,000. Carlos et al. [15] represented an integrated biochemical sensor based on a slot-waveguide micro-ring resonator which possesses *Q* factor of 1800 and *S* of 212 nm/RIU. Claes et al. [16] demonstrated a slot-waveguide-based ring resonator in SOI with the *S* of 298 nm/RIU, and Hsiao et al. [18] presented *S* of 250 nm/RIU in a slot photonic crystal ring-resonator for RI sensing, whereas the *Q* factors are limited to 1200 in [16] and 800 in [18], and Ling et al. [17] demonstrated a *Q* factor of 10^5 in polymer micro-ring resonator which achieves an acoustic sensitivity around 36.3 mV/kPa with 240 μW operating power. In order to minimize the smallest detectable wavelength shift $\Delta\lambda_{min}$ and enhance the detectable sensitivity, high *Q* cavities and a low noise detection system are required. A high *Q* factor results in narrow spectral peaks: $Q = \lambda_0/\Delta\lambda_{FWHM}$, where λ_0 and $\Delta\lambda_{FWHM}$ represent the resonance wavelength and full-width at half-maximum (FWHM) of the resonance peak, respectively. There are a number of parameters that determine the *Q* factor of cavity, such as, reduced optical losses enhance the *Q* factor, and made optical mode more localized between the ring–slot waveguide and the input/output waveguides reduces the resonance cavity losses. The last but not the least, smaller radii can increase bend losses but decrease scattering losses due to reduced round trip length.

In this paper, in order to obtain high *Q* factor sensor, a label-free RI sensor based on PhC ring–slot cavity is proposed. The proposed device consists of a photonic crystal ring–slot (PhCRS) structure, which is designed by removing six air holes in the center of structure and etching the ring–slot cavity, in which light is coupled input and output by using a PhC line defect waveguide (W1). With FDTD simulation, we adjust the ring–slot width w and the radius of the red air hole r_1 to optimize the *Q* factor and sensitivity *S*, and we show that the *Q* factor as high as 10^7 is achieved when the width (w) of ring–slot equals to $0.20a$. Compared with Refs. [14–18], the *Q* factor is enhanced by about two orders of magnitude. Even though

* Corresponding author.
E-mail addresses: hptian@bupt.edu.cn (H. Tian), jyf@bupt.edu.cn (Y. Ji).

http://dx.doi.org/10.1016/j.optcom.2014.09.014
0030-4018/

water absorption at telecom wavelength range is considered, a Q factor of $\sim$11477.3 can also be obtained when the width of ring–slot equals to 0.28a, and this width, considering the fabrication progress later, can also make the slot region to be completely filled with the glucose solution [15,16]. In order to quantitatively analyze sensitivity S of the proposed sensor device, we change the refractive index as RI=1.0, 1.30, 1.330, 1.345 and 1.377, respectively. The RI sensitivity S of 160 nm/RIU is calculated. In addition, the DL of 8.75×10^{-5} RIU is obtained. This is of extreme important in theory for label-free RI sensor to apply surface biomolecule detection.

2. Structure design of photonic crystal ring–slot cavity

The schematic view of the PhCRS structure design is shown in Fig. 1, which is based on a triangular lattice, hole-array PhC. That is because the hole-array based PhC is usually selectively removed the material underneath the cavity to form a similar free-standing membrane which can be easier to restrict the vertical leakage into the substrate than the pillar-array based PhC cavity [34]. In addition, a triangular lattice PhC can create a wider photonic band gap (PBG) than the square lattice PhC. Therefore, the structure design in this paper is based on the triangular lattice, hole-array based PhC in Fig. 1(a). In the design, triangular lattice air holes are arranged in silicon (n_{si}=3.48), in which six air holes are removed and etched the ring–slot in the center of structure. We simulate the PhCRS structure by using the open source FDTD software Meep which further divides space into a discrete grid and the fields are evolved in time using discrete time steps [40]. As a result, the grid and the time steps are made finer and finer, this becomes a closer and closer approximation for the true continuous equations. In the simulation process, The TE Gaussian-pulse source with the center frequency (ω=0.25 (2πc/a)) is used and run for several iterations. The resolution is set to 20 (that is, with a grid spacing of a/20, where a represents the lattice constant) and the time step of 0.025 a/c is employed. All the simulations are carried out with the same mesh size and time step for future comparable results. Since the boundary conditions at the spatial edges of the computational domain must be carefully considered, one-spatial unit thick perfectly matched layer (PML) which surrounds the simulated area absorbs the fields leaving the simulated region to implement reflections. Light source is placed at the head of the input line defect waveguide and monitor is placed at the end of the output line defect waveguide. By dividing the output power detected with the monitor by the input power of the source, we obtain the transmittance spectra.

As seen in Fig. 1, the lattice constant a equals to 378 nm and the air holes radius r is 0.34a (128.5 nm). Based on this structure, the transmission spectra in the PhCRS structure is shown in Fig. 2(a), and the results display obviously several different resonant modes at normalized frequencies of 0.2239 (2πc/a), 0.2493 (2πc/a), 0.304 (2πc/a), 0.313 (2πc/a), which correspond to resonant wavelengths of 1688.25 nm, 1516.25 nm, 1243.42 nm, 1207.67 nm, respectively. In order to quantitatively well analysis the properties of sensing structure, we choose the resonant frequency of 0.2493 (2πc/a) to observe the shift of resonant wavelength when refractive index near the ring–slot area and the ring–slot cavity structure are modified. Fig. 2(b) shows the steady-state electric field profile in the PhCRS structure in the x–y plane, in which the optical field is horizontally confined in the in-plane direction. However, we can also find that the confine of light need to be strengthened and the TE-like polarized light need further coupled into the ring waveguide in-plan direction.

3. Simulation results and discussion

3.1. The simulation analysis of Q factor and sensitivity S in PhCRS structure

The Q factor of a cavity is determined by the energy loss per cycle versus the energy stored. The energy loss mainly includes reflection loss and the absorption loss of cavity material. Therefore, to improve the Q factor of the PhCRS structure design, we should decrease the energy loss. With the PhCRS structure, the Q factor can be expressed as follows: [2,3]

$$\frac{1}{Q}=\frac{1}{Q_c}+\frac{1}{Q_{loss}} \tag{1}$$

Where Q_c represents the lifetime, that is, the time of light can decay from the cavity into the waveguide, and Q_{loss} refers to the material absorption and optical radiation from the cavity into the surrounding air. Eq. (1) gives an important hint that suppressing radiation loss can enhance the Q factor. Therefore, we adjust the cavity structure and make that the electric field profile of cavity edges should not be abrupt but gentle so that the energy loss per cycle versus the energy stored is lower. Here the strategy to alter the ring–slot width w and the radius of the red air hole r_1 makes confinement gentler and obtains high Q factor. When we change the ring–slot width and the radius of red air hole near the cavity edge, the Bragg reflection effect in multiple directions can be modified. Because the phases of partial refection at the cavity edges are modified, the resultant phase-mismatch weakens the magnitude of Bragg reflection. To compensate for the reduction of the reflection, light is considered to penetrate more inside the mirror and be reflected perfectly. This means that the electric field profile at the cavity edges becomes gentler. With the appropriate alteration, the profile is considered to be close to the ideal confinement expressed by the Gaussian function [1]. Using this

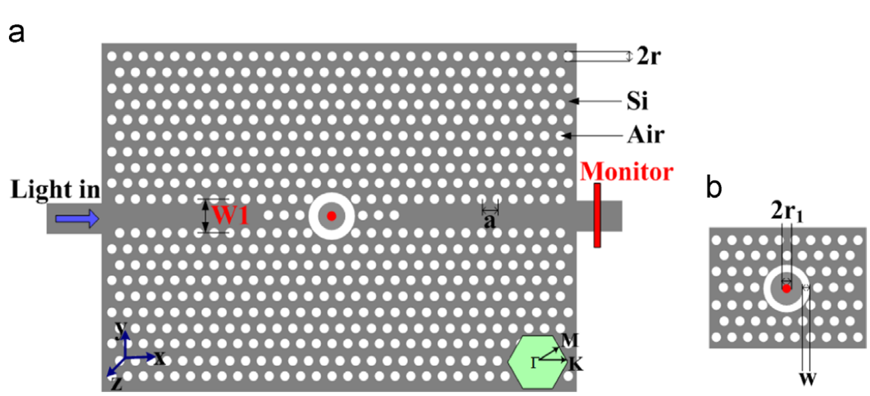

Fig. 1. The photonic crystal ring–slot (PhCRS) structure design using a 2D photonic-crystal. (a) Schematic of the base cavity structure with triangular lattice of air holes, where a=378 nm, r=0.34a, $W_1=\sqrt{3}a$. (b) Designed cavity structure created by altering the ring–slot width w and the radius r_1.